# Photolysis of Methanol at 185 nm. Quantum Mechanical Calculations and Product Study

**R. J. Buenker,*† G. Olbrich,‡ H.-P. Schuchmann,‡ B. L. Schürmann,† and C. von Sonntag*‡**

*Contribution from the Lehrstuhl für Theoretische Chemie der Universität-Gesamthochschule Wuppertal, D-5600 Wuppertal 1, West Germany, and the Max-Planck-Institut für Strahlenchemie, D-4330 Mülheim a.d. Ruhr, West Germany.* *Received August 3, 1983*

**Abstract:** A series of ab initio MRD-CI calculations is carried out in conjunction with new experimental investigations in order to study the photolysis of methanol in its $^1$(n–3s) excited state at 185 nm. Potential surfaces for the key primary processes of O–H, C–O, and C–H scission are obtained as well as for the $H_2$ elimination reaction which leads to formaldehyde production. Comparison with known transition and dissociation energy data indicates that the present calculations are accurate to within 0.1 eV over the entire potential surface of interest in this study. In agreement with the recent work of Kassab et al. it is found that O–H scission proceeds along a purely repulsive pathway corresponding to the conversion of the 3s Rydberg orbital into a 1s AO of the hydrogen atom, but when the C–O bond is broken a new feature is found, namely a slight barrier for this process caused by a sharply avoided crossing between the respective Rydberg and valence electronic configurations in this case. The fact that the mass of the hydrogen atom fragment is much smaller than that of either the methyl or hydroxyl radicals tends to further promote O–H scission over the corresponding C–O bond-breaking process, in agreement with known quantum yield results for the photolysis of saturated alcohols; this mass effect is confirmed by new experimental evidence also obtained in the present study which shows that the quantum yields of C–O scission products are enhanced by deuteration at the oxygen atom of methanol. Finally, the calculations indicate that $H_2$ elimination proceeds with a slight barrier in the excited-state potential curve, quite possibly involving a nonconcerted mechanism in which the O–H bond is first lengthened substantially before a second hydrogen atom is abstracted from the carbon atom of the same molecule.

## I. Introduction

The first absorption band of saturated alcohols has been attributed to an n-Rydberg transition,[1,2] similar to that for the water molecule. The maximum intensity for this system lies in the neighborhood of 185 nm, which is a wavelength of the Hg low-pressure arc. The photolysis of primary and secondary alcohols at 185 nm leads to the same main products in both the liquid and gas phases, namely hydrogen, the corresponding carbonyl compound, and certain dehydro dimers (for reviews on this topic see ref 3 and 4). Product analysis, including species derived from deuterated compounds, indicates that there are two major primary processes that appear to dominate, namely homolytic scission of the O–H bond, e.g.

$$CH_3OH^* (n \rightarrow 3s) \rightarrow CH_3O\cdot + H\cdot \quad (1)$$

and elimination of a single molecule of hydrogen, e.g.

$$CH_3OH^* \rightarrow CH_2O + H_2 \quad (2)$$

Homolytic cleavage of the C–O bond, e.g.

$$CH_3OH^* \rightarrow \cdot CH_3 + \cdot OH \quad (3)$$

is always a minor process, as is the scission of a C–H bond, e.g.

$$CH_3OH^* \rightarrow \cdot CH_2OH + H\cdot \quad (4)$$

or of analogous C–C bonds (cf. ethanol[5] and 2-propanol[6,7]). These results for alcohols stand in some contrast to what is observed for saturated ether compounds, despite the fact that the first absorption band in these systems also corresponds to an n-Rydberg transition,[1,2] since 185-nm photolysis of ethers leads mainly to scission of a C–O bond.[3,4] Especially considering the fact that in the ground state of alcohols the C–O bond is notably weaker than the O–H bond, the question has arisen quite naturally as to why scission of the C–O bond is apparently of so little importance in the photolysis of these systems.

Since methanol[8-10] is characterized by the same trends as those described above for saturated alcohols in general, there seemed to be a good possibility that accurate ab initio CI methods could be applied quite effectively toward the understanding of these photolysis results, since systems with only two non-hydrogenic atoms lie well within the range of applicability generally attributed to such theoretical methods. The present contribution reports the results of a series of CI calculations for the energy hypersurface of methanol in both its ground and lowest lying singlet excited state. These data are then compared with known experimental findings for the photolysis of saturated alcohols and ethers, including some new measurements which were suggested in part upon consideration of the calculated results. After the present calculations had been completed, a paper by Kassab, Gleghorn, and Evleth appeared which also deals with theoretical aspects of methanol photochemistry,[11] and quantitative comparison with the results of these calculations will also be undertaken in the course of this study.

## II. Details of the CI Potential Surface Calculations and Other Theoretical Considerations

The Cartesian Gaussian AO basis set employed in the present study is of double-ζ-plus-polarization quality including Rydberg s and p functions located at the oxygen atom of methanol. The DZ portion of the basis is taken from the work of Huzinaga[12] and Dunning[13] for the carbon and oxygen species and the {4,1} contraction for the hydrogen s AO's given by Peyerimhoff et al.[14]

†Lehrstuhl für Theoretische Chemie der Universität-Gesamthochschule Wuppertal.
‡Max-Planck-Institut für Strahlenchemie.

(1) Robin, M. B. "Higher Excited States of Polyatomic Molecules"; Academic Press: New York, Vol. 1, p 254.
(2) Sandorfy, C. *Top. Curr. Chem.* **1979**, *86*, 91-138.
(3) von Sonntag, C.; Schuchmann, H.-P. *Adv. Photochem.* **1977**, *10*, 59-145.
(4) von Sonntag, C.; Schuchmann, H.-P. In "The Chemistry of Functional Groups"; Patai, S. Ed.; Wiley: Chichester, 1980; Supplement E, pp 903-922.
(5) von Sonntag, C. *Z. Phys. Chem. (Wiesbaden)* **1970**, *69*, 292-304.
(6) von Sonntag, C. *Z. Naturforsch., B* **1972**, *27B*, 41-46.
(7) von Sonntag, C. *Tetrahedron* **1968**, *24*, 117-121.
(8) Porter, R. P.; Noyes, W. A., Jr. *J. Am. Chem. Soc.* **1959**, *81*, 2307-2311.
(9) Hagège, J.; Roberge, P. C.; Vermeil, C. *J. Chim. Phys. Phys.-Chim. Biol.* **1968**, *65*, 641-647. Hagège, J.; Roberge, P. C.; Vermeil, C. *Ber. Bunsenges. Phys. Chem.* **1968**, *72*, 138-146. Hagège, J.; Leach, S.; Vermeil, C. *J. Chim. Phys. Phys.-Chim. Biol.* **1965**, *62*, 736-746. Hagège, J.; Roberge, P. C.; Vermeil, C. *Trans. Faraday Soc.* **1968**, *64*, 3288-3299.
(10) Herasymovych, O. S.; Knight, A. R. *Can. J. Chem.* **1973**, *51*, 147-148.
(11) Kassab, E.; Gleghorn, J. T.; Evleth, E. M. *J. Am. Chem. Soc.* **1983**, *105*, 1746-1753.
(12) Huzinaga, S. *J. Chem. Phys.* **1965**, *42*, 1293-1302.
(13) Dunning, T. H. *J. Chem. Phys.* **1976**, *65*, 3854-3862.
(14) Peyerimhoff, S. D.; Buenker, R. J.; Allen, L. C. *J. Chem. Phys.* **1966**, *45*, 734-749.

0002-7863/84/1506-4362$01.50/0 

**Table I.** Technical Details of MRD-CI Calculations for Various States

| state | electronic config | MO basis | SAFT/SAF[a] | $E_{SCF}$ | $E_{CI(T=0)}$ | $\Delta E_{full\ CI}^{cor}$ | *n* mains/ *n* roots |
|---|---|---|---|---|---|---|---|
| $^1A'$ | $...(6a')^2(7a')^2(1a'')^2(2a'')^2$ | $^1A'$ | 17559/2534 | −115.0348 | −115.2687 | −0.0156 | 1/1 |
| $^1A''$ | $(7a')^2(8a')^1(1a'')^2(2a'')^1$ | $^1A''$ | 39648/2425 | −114.8066 | −115.0173 | −0.0120 | 1/1 |
| $^3A''$ | $(7a')^2(8a')^1(1a'')^2(2a'')^1$ | $^3A''$ | 66294/2338 | −114.8133 | −115.0245 | −0.0108 | 1/1 |
| $^1A''$ | $(7a')^2(9a')^1(1a'')^2(2a'')^1$ | $^1A''$ | 39648/2414 | −114.8057 | −114.9777 | −0.0167 | 1/1 |
| $^3A''$ | $(7a')^2(9a')^1(1a'')^2(2a'')^1$ | $^3A''$ | 72864/2332 | −114.8133 | −114.9849 | −0.0176 | 1/1 |
| $^1A'$ | $(6a')^2(7a')^1(9a')^1(1a'')^2(2a'')^2$ | $^3A'$ | 38878/2424 | −114.7505 | −114.9024 | −0.0200 | 1/1 |
| $^3A'$ | $(6a')^2(7a')^1(9a')^1(1a'')^2(2a'')^2$ | $^3A'$ | 64544/2247 | −114.7505 | −114.9039 | −0.0199 | 1/1 |
| $^1A''$, (C—O = 3.0 Å) | $(7a')^2(9a')^1(1a'')^2(2a'')^1$ | $^1A''$ | 260729/1821 | −114.9407 | −114.8997 | −0.0201 | 4/1 |
| $^1A''$, (C—O = 2.0 Å) | $(7a')^2(9a')^1(1a'')^2(2a'')^1$ | $^1A''$ | 260729/2226 | −114.8857 | −114.9624 | −0.0201 | 4/1 |
| $^1A''$, (C—O = 1.6 Å) | $(7a')^2(8a')^1(1a'')^2(2a'')^1$ | $^1A''$ | 39648/2666 | −114.8033 | −115.0175 | −0.0143 | 1/1 |
| $^1A''$, (C—O = 4.0 Å) | $(7a')^2(1a'')^2(2a'')^2$ | $^3A'$ | 38878/1426 | −114.9441 | −115.1447 | −0.0137 | 1/1 |
| $^1A''$, (O—H = 1.4 Å) | $(7a')^2(9a')^1(1a'')^2(2a'')^1$ | $^1A''$ | 221149/4582 | −114.8495 | −114.9147 | −0.0210, 2*R* | 5/2 |
| | | | | | −115.0612 | −0.0137, 1*R* | |

[a] SAFT = symmetry-adapted functions total; SAF = symmetry-adapted functions, after selection (see also ref 16–18).

To introduce polarization in the basis a p function was placed on each H atom with an exponent of $\alpha = 0.735$; the diffuse function exponents are 0.020 and 0.012 for the s-type and 0.015 and 0.009 for the p-type Rydberg species. The total (DZP) AO basis thus consists of 48 functions, although for the purposes of carrying out certain of the geometrical optimizations a smaller (DZ) set in which the hydrogen p functions are deleted has also been employed. The latter DZ set is very similar to the largest AO basis employed in the work of Kassab et al.,[11] except for some minor differences in the choice of exponents for the various diffuse functions.

The initial calculations with the DZP basis were carried out for the equilibrium ground-state geometry of methanol, as given by Gerry et al.:[15] $R_{O-H} = 1.0936$ Å, $R_{O-H} = 0.9451$ Å, $R_{C-O} = 1.4246$ Å, ∠HCH = 108° 38′, ∠COH = 108° 32′, and angle of methyl tilt of 3° 16′. The ground-state SCF energy in the RHF formalism is −115.03484 hartree in this basis. The corresponding CI treatment is of the multireference single- and double-excitation (MRD-CI) variety employing configuration selection and energy extrapolation,[16-18] details of which may be found in the original references (a core of two 1s orbitals is maintained throughout the treatment). Typical sizes of the selected CI spaces treated explicitly in this study for various electronic states and nuclear geometries are given in Table I: parent state SCF MO's are generally employed except where stated otherwise. The CI spaces treated thereby are considerably larger than in the work of Kassab et al.,[11] in which secular equations falling in the order of 100–400 have been solved. The transition energies to the lowest excited states of methanol and its positive ion obtained at both the SCF and CI levels agree well with the corresponding experimental data for this (vertical) spectrum. Since methanol is a saturated system the lowest excited states are all of Rydberg character, of which the 3s and 3p species originate from the highest two occupied MO's of the ground state, 7a′ and 2a″ (n). The n → 3s singlet–singlet bands are centered at 6.84 eV according to the calculations, or 181 nm, in good agreement with measured data (182 nm) (a lower value of 6.5 eV is found in the calculations of ref 11). The IP results are only slightly less satisfactory in the present CF treatment (0.4–0.5 eV too low, which is normal for this type of AO basis), indicating that the present theoretical treatment is quite adequate at least in the neighborhood of the ground-state equilibrium geometry.

**A. Potential Surface Calculations.** As discussed in the Introduction there are four primary processes which should be considered in connection with the photolysis of methanol (eq 1–4), three of which involve simple breaking of the O–H, C–O, and C–H bonds of the molecule. To study the latter reaction types the respective bond distances have simply been increased systematically relative to their ground-state equilibrium values, while holding all other structural parameters fixed in each case. The first such potential curves are given in Figure 1 for the O–H dissociative processes in both the ground and lowest lying singlet excited states. The lowest direct dissociation products are the methoxyl radical plus hydrogen atom in their respective ground states. An important aspect of this process is the fact that the $CH_3O$ ground state is (spatially) doubly degenerate, with the odd electron having a choice between the two different oxygen lone pairs. As a result both the methanol ground and lowest lying excited singlet states correlate with these products. The ground-state O–H dissociation energy is computed to be 4.33 eV in the CI calculations, in very good agreement with the corresponding experimental findings[19] (4.37 eV), again indicating that the theoretical treatment is of suitable accuracy over the entire range of nuclear geometries of interest in this study. The less extensive CI calculations of Kassab et al.[11] obtain a much smaller value of 3.5 eV for this quantity so that it would appear a much higher degree of quantitative reliability can be attributed to the potential surfaces computed in the present study.

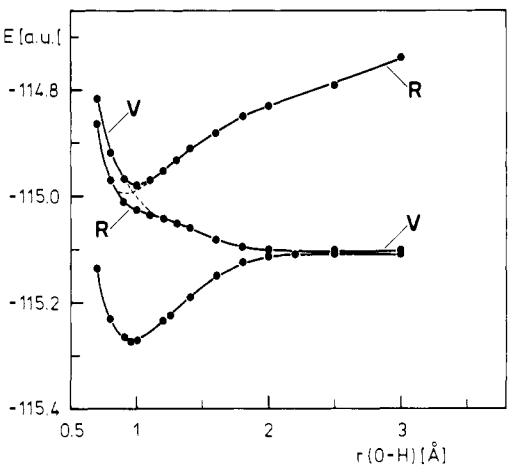


**Figure 1.** Potential curves for the O–H bond-breaking process: $^1A'$ (ground state), $^1A''$ (3s), $^1A''$ ($3p_x$). The dotted lines show the conceptual behavior of diabatic surface; see text for explanation. In this connection note that the designation V (for valence) in the uppermost state at short bond distances is only schematic; in reality the valence character is distributed among higher-lying Rydberg states in this region.

The upper orbital in the lowest singlet excited state undergoes a gradual transformation from a 3s Rydberg species in the vertical excitation region to a pure hydrogen 1s AO at the dissociation limit. This behavior is best understood in terms of a relatively strongly avoided crossing involving Rydberg–valence (R–V) mixing

(15) Gerry, M. L. C.; Lees, R. M.; Winnewisser, G. *J. Mol. Spectrosc.* **1976**, *61*, 231–242.
(16) Buenker, R. J.; Peyerimhoff, S. D. *Theor. Chim. Acta* **1974**, *35*, 33–58.
(17) Buenker, R. J.; Peyerimhoff, S. D. *Theor. Chim. Acta* **1975**, *39*, 217–228.
(18) Buenker, R. J.; Peyerimhoff, S. D.; Bruna, P. J. In "Computational Theoretical Organic Chemistry"; Csizmadia, I. G., Daudel, R., Eds.; Reidel: Dordrecht, 1981; p 55–76.
(19) Harding, L. B.; Schlegel, H. B.; Krishnan, R.; Pople, J. A. In "Potential Energy Surfaces and Dynamics Calculations"; Truhlar, D. G., Ed.; Plenum Press: New York, 1980; pp 169–183 and references therein.

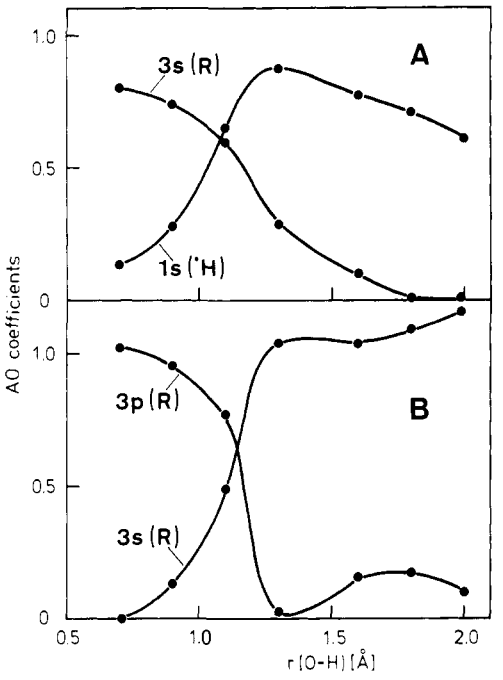


**Figure 2.** Rydberg–valence mixing demonstrated by the variation of AO coefficients as a function of the O–H distance in the weakly avoided crossing region. (A) AO analysis for the lower $^1A''$ (3s); (B) AO analysis for the upper $^1A''$ ($3p_x$) state.

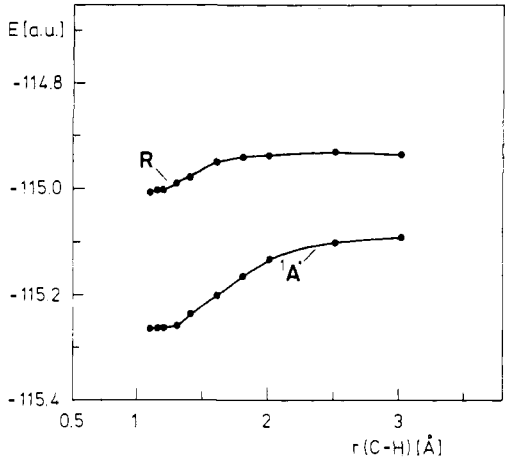


**Figure 3.** Potential curves of the $^1A'$ and $^1A''$ states for the C–H stretching coordinate.

of a type well-known for smaller systems.[20-24] A plot of the AO contribution to this MO in both the lowest singlet excited states contained in Figure 2 illustrates this situation more quantitatively. The change in character occurs relatively slowly, which is consistent with the fairly strong avoidance of the R–V potential curves seen in Figure 1. As a consequence of the latter the lower excited-state potential curve is everywhere repulsive, showing only a tendency toward shoulder formation in the immediate region of the R–V crossing. The total lack of an activation barrier for

(20) Mulliken, R. S. *Int. J. Quantum Chem.* **1971**, *5*, 83–98.
(21) Sandorfy, C. In C. Sandorfy, P. J. Ausloos and M. B. "Chemical Spectroscopy and Photochemistry in the Vacuum Ultraviolet"; Sandorfy, C., Ausloos, P. J., Robin, M. B., Eds.; Reidel: Dordrecht 1974; p 149.
(22) Buenker, R. J.; Peyerimhoff, S. D. *Chem. Phys. Lett.* **1975**, *36*, 415–422.
(23) Runau, R.; Peyerimhoff, S. D.; Buenker, R. J. *J. Mol. Spectrosc.* **1977**, *68*, 253–268.
(24) Evleth, E. M.; Gleghorn, J. T.; Kassab, E. *Chem. Phys. Lett.* **1981**, *80*, 558–563. These authors prefer to speak of this phenomenon as the Rydberg initation, that is, as a gradual transformation between a valence and a Rydberg orbital along the reaction coordinate. In fact the two ideas are equivalent, deRydbergization being a special case of Rydberg–valence avoided crossing in which the two configurations differ by only a single excitation (so that the transformation can occur at the Hartree–Fock level).

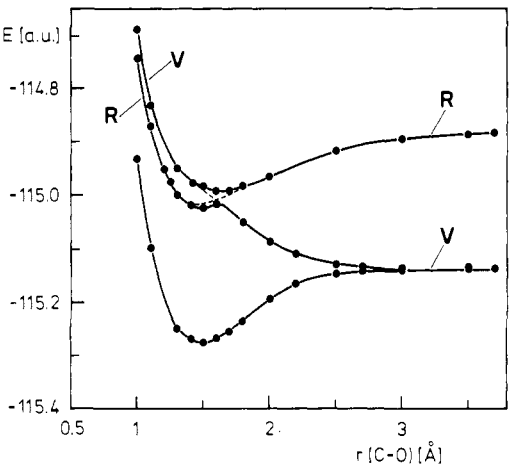


**Figure 4.** Potential curves for the C–O bond-breaking process: $^1A'$ (ground state), $^1A''$ (3s), $^1A''$ ($3p_x$). See additional remarks appended to Figure 1.

this reaction, as also noted by Kassab et al.,[11] is clearly consistent with the general experimental findings noted for photolysis of saturated alcohols in which O–H homolytic scission is found to be a dominant process, but to obtain a firm theoretical explanation of these phenomena it is clearly necessary to obtain analogous data for competing reaction pathways.

The potential curves for C–H scission are qualitatively quite different, as can be seen from Figure 3. The major difference between these data and those for O–H stretch in Figure 1 is clearly the fact that in the present case the methanol ground and lowest excited states correlate with different dissociation products, with the hydroxymethyl radical being a spatially nondegenerate species unlike the methoxy radical. The n → 3s excited state thus needs to overcome a sizeable barrier (~35 kcal mol$^{-1}$) in Figure 3 in order to break a C–H bond. The products are $\cdot CH_2OH^* + H\cdot$, corresponding to an e → p$\sigma$ promotion in the methyl radical or in ammonia, for example. Thus, although the C–H and O–H ground-state dissociation processes for alcohols are quite similar in character, a large distinction is apparent in the n → 3s excited species, thereby easily explaining the almost total aversion to C–H scission observed in the photolysis experiments for such systems (see also the discussion of Kassab et al.[11]).

The third type of simple bond-breaking process for methanol is represented by the C–O potential curves of Figure 4. In this case the lowest dissociation products are the methyl and hydroxyl radicals in their respective ground states. Since the hydroxyl radical is spatially degenerate ($^2\Pi$), the situation is qualitatively similar to the O–H dissociation, with both the ground and lowest excited n → 3s methanol states correlating with the same fragment species. The calculated dissociation energy for this process (3.74 eV without geometry optimization for the fragments) is found to be in good agreement with the experimental value of 3.91 eV, so that again the indication is that the present level of theoretical treatment achieves a good degree of balance between ground and low-lying excited states over the entire range of nuclear geometries thought to be involved in the methanol photolysis experiments. Because the C–O bond is 26 kcal mol$^{-1}$ weaker than the corresponding O–H bond, the exothermicity of the photochemical dissociation is significantly greater in the present case, but a more critical distinction between these two primary processes is found in the nature of their respective Rydberg–valence avoided crossings, which occur in the neighborhood of the vertical geometry (Figure 4).

From the point of view of qualitative MO theory the R–V mixing description would appear to be quite similar in the C–O and O–H bond-breaking processes, in the former case involving a gradual transition from a 3s Rydberg species to the 2p$\sigma$ methyl valence orbital instead of the 1s hydrogen AO in O–H scission. Comparison of the variation of these AO contributions to the HOMO of the excited methanol singlet as a function of the C–O distance in Figure 5 with the analogous results in Figure 2 shows

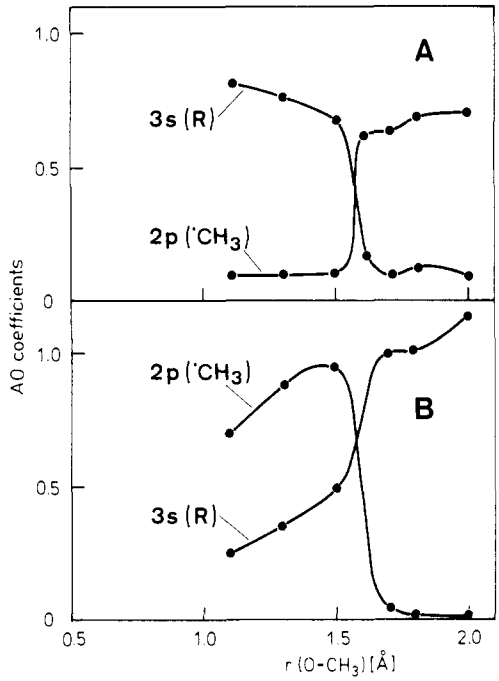


**Figure 5.** Variation of AO coefficients in the avoided crossing region of the $^1A''$ (3s) and $^1A''$ ($3p_x$) potential curves for the C–O stretching coordinate. (A) AO analysis of the (lower) $^1A''$ (3s) state; (B) AO analysis of the (upper) $^1A''$ ($3p_x$) state.

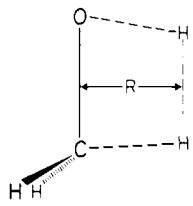


**Figure 6.** Graphical representation of the reaction coordinate $R$, chosen for the reaction given in Figure 7.

that the orbital transformation occurs significantly more rapidly, i.e., over a smaller range of internuclear distances, in this case than in the O–H example, so that a more sharply avoided crossing and, correspondingly, a smaller barrier in the lowest excited state occurs under that C–O stretch. In the Born–Oppenheimer approximation there is thus a clear difference between the C–O and O–H dissociation processes for methanol in its n → 3s excited singlet state, but in view of the fact that the next excited state of the same symmetry has an energy which is less than 0.5 eV higher at the closest point of approach of their potential curves, it is advisable to withhold judgment on the experimental consequences of this finding until the possible effects of nonadiabatic coupling have also been considered.

Before this point is addressed, however, potential curves for the second primary process mentioned in the introduction, namely the elimination of a single molecule of $H_2$ and simultaneous production of formaldehyde (eq 2), should be considered, especially since it appears to be of comparable importance to O–H scission based on product analysis reported for the photolysis reactions of saturated alcohols. Since there is no a priori conception about the geometrical details of the elimination reaction, the following model was constructed. First, the two hydrogen atoms to be eliminated, namely that from the hydroxyl group and one from the methyl group, were taken to be coplanar with the carbon and oxygen atoms. The reaction coordinate was chosen to be the distance $R$ between the C–O bond and the H–H species being formed, which in turn were kept parallel throughout the course of the elimination (see Figure 6). The starting point of the reaction was the methanol molecule in its equilibrium geometry, for which $R$ has a value of about 1.0 Å. The end point of the reaction was then defined to be a formaldehyde molecule and

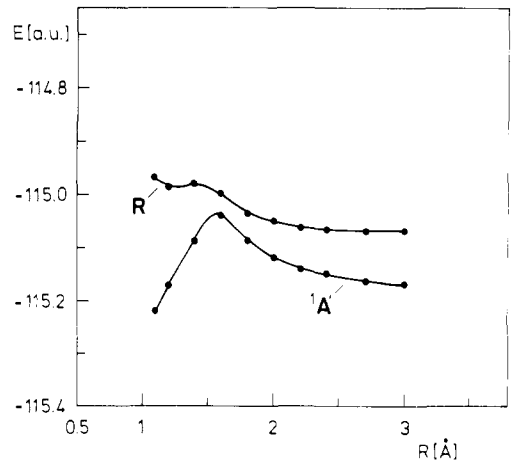


**Figure 7.** Suggested reaction pathway for the creation of formaldehyde; potential curves of the ground state and first (n–3s) excited state.

diatomic hydrogen in their respective equilibrium geometries separated by a distance of $R$ = 10.0 Å. As a first guess for the Cartesian coordinates of the various atoms at intermediate geometries, interpolation between the methanol ground-state conformation and the above end point was employed. The other two methyl hydrogens were taken to vary linearly with $R$ while an exponential dependence on $R$ was assumed for both the C–O and the H–H bond lengths. On the basis of these interpolated coordinates, the bond distance of the hydrogen molecule being formed and the location of its midpoint were optimized in the n–3s Rydberg state for values of $R$ between 1.0 and 3.0 Å. Since for values of $R$ = 1.2 and 1.4 Å the optimization failed, the initial coordinates obtained by interpolation were used. In all the calculations pertaining to the hydrogen elimination the p functions on the hydrogen atoms were deleted from the previous AO basis; this change had only a minimal effect on the computed vertical spectrum of methanol relative to the values reported in Table I.

The resulting MRD-CI potential curves for the $H_2$ elimination reactions of methanol in both its ground and n–3s singlet excited states are given in Figure 7. These results are quite different as compared to any of the single bond-breaking processes discussed earlier. The main difference lies in the fact that the ground-state curve possesses a maximum at $R$ = 1.6 Å, corresponding to an activation energy of 4.89 eV. The n–3s excited-state energy decreases at first, but then approaches a maximum at about the same value of $R$ (1.6 Å), from which point onward the energy again decreases monotonically until it reaches an asymptote corresponding to the $H_2CO$ $^1(n,\pi^*)$ state plus ground-state $H_2$. As can be deduced from the calculated bond lengths the $H_2$ molecule is already formed at a value of $R$ = 1.6 Å, and the decrease of the energy from this point on may be attributed to structural relaxation and closed-shell repulsion. In a sense the present elimination reaction is similar to the C–H scission process (Figure 3) discussed earlier, since the fragment system is again nondegenerate. A major difference between these two cases is noted in the energy splittings between ground and excited states, becoming a small as 20 kcal mol$^{-1}$ in the $H_2$ elimination but never dropping below 90 kcal mol$^{-1}$ for the C–H scission. In the strict adiabatic approximation (infinite nuclear masses) one would conclude that in the $^1(n,3s)$ state of methanol a slight barrier to elimination is encountered, depending on which vibrational level is reached after the initial excitation; the products of the reaction are not $H_2CO$ and $H_2$ in their respective ground states, but rather excited formaldehyde and $H_2$. Since the products of the methanol photolysis include a rather high percentage of ground-state $H_2CO$, it appears that surface-hopping effects between ground and excited states (note that the symmetries of these states do become the same in more distorted geometries than those considered explicitly in the present work) may play an important role in the description of this process.

**B. Dynamical Considerations: Nuclear Mass Effects.** Although a complete dynamical treatment of the methanol photolysis re-

action is not feasible at the present time, there are several qualitative points which would clearly have a bearing on such an investigation and which should be kept in mind in formulating a theoretical interpretation of these phenomena. The potential surface calculations of the preceding subsection indicate that in several of the possible primary processes nonadiabatic effects may play an important role. The various avoided crossings indicated in these results suggest strongly that predissociation effects involving surface hoppings of one form or another have a bearing on the quantum yields of the various products observed experimentally in the photolysis of methanol, and saturated alcohols and ethers in general. The probability that a given reaction channel is favored therefore is determined to a good degree by the relative velocities of the molecular species involved. A particularly striking confirmation of the importance of such kinetic considerations can be seen in the appearance of the X$\alpha$ and X$\beta$ bands of HCN and DCN, respectively.[25] The upper states in these transitions are strongly predissociated leading to decomposition into H + CN; potential curves explicitly predicting this type of activity have been obtained via ab initio CI calculations.[26] The predissociative character in this system is manifested experimentally in the diffuseness of the associated spectral bands, but the effect is much more pronounced in HCN than in DCN,[25] demonstrating that the lighter H atom can much more readily make the transition from the bound potential curve initially reached upon irradiation of the molecular ground state to the dissociative channel than can the deuteron.

In the case of the methanol photolysis the above considerations can be made somewhat more quantitative by assuming the following simple model for a competition between several dissociative channels. If the combined system is initially at rest at the top of a barrier (or at the start of a repulsive branch) with a potential difference $\Delta E$ separating it from the fragments in a given channel, the laws of conservation of energy and momentum require that the velocity of a given product species is $V_i = \{2\Delta E m_j/(m_i + m_j)m_i\}^{1/2}$, where $m_i$ and $m_j$ are the masses of the two departing fragments. The speed with which a given dissociative process occurs is thus determined to a large extent by the mass of the lighter of the particles in the exit channel. In the present context the above model indicates that decompositions involving hydrogen atoms have an advantage over related processes in which the masses of the product species are more nearly equal, favoring the O–H scission reaction over the process in which the C–O bond is broken, for example. Such kinetic aspects of the present calculations must be weighed along with the potential surface results of Figures 1, 3, 4, and 6 in trying to understand the details of the product quantum yields in these photochemical reactions.

## III. Experimental Observations for the Photolysis of Methanol and O-Deuterated Methanol

Given the theoretical results of the preceding section it was decided to take a closer look at the 185-nm photolysis of methanol as a prototype for photodecomposition of saturated alcohols, including the study of isotopically substituted methanol $CH_3OD$. In order to avoid a decomposition of vibrationally hot intermediates which might be formed upon photolysis this study has been undertaken in the liquid phase since vibrational relaxation occurs considerably faster under these conditions than in the gas phase. As a result it is often found that the products of liquid-phase photolysis are more easily interpretable in terms of primary processes than are their counterparts in gas-phase experiments, even though effects peculiar to liquids such as hydrogen bonding can lead to additional complications.[27] Fortunately the methanol system appears to behave similarly in both the gas[8] and the neat liquid phase.[28] Consequently, comparison between quantum mechanical calculations (which directly apply only to gas-phase conditions) and experimental results obtained in the liquid phase should still be realistic.

**Table II.** Photolysis (185 nm) of Liquid MeOH and MeOD: Products and Quantum Yields

| | MeOH | MeOD |
|---|---|---|
| $H_2$ | 0.78 ± 0.01 | ≤0.01 |
| HD | | 0.76 ± 0.01 |
| CO | 0.001 | |
| methane | 0.035 | 0.050 |
| ethane | 0.005 | 0.007 |
| formaldehyde | 0.29 ± 0.03 | 0.31 ± 0.03 |
| ethanol | $0.02_5$ | $0.02_5$ |
| ethylene glycol | not determined | |

**Table III.** Free-Radical Processes in the 185-nm Photolysis of Methanol

| | |
|---|---|
| $CH_3O\cdot + CH_3OH \rightarrow CH_3OH + \cdot CH_2OH$ | (5) |
| $\cdot H + CH_3OH \rightarrow H_2 + \cdot CH_2OH$ | (6) |
| $\cdot CH_3 + CH_3OH \rightarrow CH_4 + \cdot CH_2OH$ | (7) |
| $\cdot OH + CH_3OH \rightarrow H_2O + \cdot CH_2OH$ | (8) |
| $2CH_3O\cdot \rightarrow CH_2O + CH_3OH$ | (9) |
| $CH_3O\cdot + \cdot CH_2OH \rightarrow CH_2O + CH_3OH$ | (10) |
| $2\cdot CH_2OH \rightarrow CH_2OH\text{-}CH_2OH$ | (11) |
| $2\cdot CH_2OH \rightarrow CH_2O + CH_3OH$ | (12) |
| $\cdot CH_3 + \cdot CH_2OH \rightarrow CH_3\text{-}CH_2OH$ | (13) |
| $\cdot CH_3 + \cdot CH_2OH \rightarrow CH_4 + CH_2O$ | (14) |
| $2\cdot CH_3 \rightarrow CH_3\text{-}CH_3$ | (15) |

Products (except ethylene glycol; see below) and their quantum yields are given in Table II. The hydrogen formed in the case of $CH_3OD$ consists practically only of HD (≥98% HD, ≤2% $H_2$, traces of $D_2$). There is good agreement on $\phi(H_2)$, $\phi(CH_4)$, and $\phi(C_2H_6)$ with an earlier study,[28] but there are discrepancies regarding $\phi(CH_2O)$ and $\phi(CH_2OH\text{–}CH_2OH)$. The reasons for this are only partly understood, but we feel that the present study has yielded more reliable data. The $H_2$ content of the hydrogen formed upon photolysis of $CH_3OD$ is now much smaller than had been found earlier,[28] and this is thought to be due to the higher degree of deuteration in the $CH_3OD$ used in the present study.

Some of the products can be measured with good accuracy and can serve as key products to distinguish between the photolysis of $CH_3OH$ and $CH_3OD$. These are hydrogen, methane, and ethane.

In order to relate the products to primary processes one must consider the free-radical reactions that are undergone by the radicals formed in reactions 1, 3, and 4. They are compiled in Table III. The most reactive radicals in this system are the OH radical and the H atom. They abstract carbon-bound H atoms almost exclusively (reactions 8 and 6; $k_8 = 7 \times 10^8$ $M^{-1}$ $s^{-1}$,[29] $k_6 = 2 \times 10^6$ $M^{-1}$ $s^{-1}$ [30]) under our experimental conditions. The methoxyl radical is somewhat less reactive ($k_5 = 2.6 \times 10^5$ $M^{-1}$ $s^{-1}$ [31]). Under the present experimental conditions these three radicals all exclusively undergo the hydrogen abstraction reactions and do not enter into radical–radical reactions. For this reason reactions 9 and 10 can be neglected as a source of formaldehyde, one of the main products. A brief estimate confirms this statement. If we consider that all radical–radical reactions occur in the small layer into which the light penetrates, the reaction volume is the cell surface multiplied by penetration depth (to 90% absorption). The extinction coefficient of liquid methanol at 185 nm is around 6 $M^{-1}$ $cm^{-1}$.[32] Thus, in neat methanol (25 M) 90% absorption is reached within 70 $\mu$m. At a flux of $1 \times 10^{16}$ quanta $s^{-1}$ $cm^{-2}$, taking a diffusion-controlled rate of the bimolecular decay of

(25) Herzberg, G.; Innes, K. K. *Can. J. Phys.* **1957**, *35*, 842–879.
(26) Perič, M.; Peyerimhoff, S. D.; Buenker, R. J. *Can. J. Chem.* **1977**, *55*, 1533–1545.
(27) Schuchmann, H.-P.; von Sonntag, C.; Schulte-Frohlinde, D. *J. Photochem.* **1975**, *4*, 63–74.
(28) von Sonntag, C. *Tetrahedron* **1969**, *25*, 5853–5861.
(29) Farhataziz; Ross. A. B. "Selected Specific Rates of Reactions from Transients from Water in Aqueous Solution. III. Hydroxyl Radical"; American Chemical Society: Washington, DC, 1977; NSRDS-NBS59.
(30) Anbar, M.; Farhataziz; Ross, A. B. "Selected Specific Rates of Reactions of Transients from Water in Aqueous Solution. II. Hydrogen Atom"; American Chemical Society: Washington, DC, 1975; NSRDS-NBS51.
(31) Ellison, D. H.; Salmon, G. A.; Wilkinson, F. *Proc. R. Soc. London, Ser. A*, **1972**, *A328*, 23–36.
(32) Weeks, J. C.; Meaburn, G. M. A. C.; Gordon, S. *Radiat. Res.* **1963**, *19*, 559–567.

radicals ($k = 10^9$ $M^{-1}$ $s^{-1}$) and random distribution, the steady-state radical concentration in the reaction volume is estimated at about $2 \times 10^{-6}$ M. This steady-state concentration is too low by a factor of more than $10^3$ to allow reactions 9 and 10 to become significant in competition with reaction 5.

The termination of the most abundant radical, the hydroxymethyl radical, yields practically only ethylene glycol (reaction 11), the disproportionation reaction 12 being of little importance.[33] The methyl radical can undergo four reactions. Hydrogen abstraction yields methane (reaction 7); combination with the hydroxylmethyl radical affords ethanol (reaction 13). The alternative disproportionation (reaction 14) is of little importance, as shown by the low yield of $CH_3D$ from $CH_3OD$.[28] The combination of two methyl radicals gives rise to ethane (reaction 15). The water formed in reaction 8 cannot be measured at the small turnovers employed in the present work, but for the elucidation of the mechanism this is not necessary.

The fact that $CH_3OD$ yields practically no $H_2$ (Table II) points to the absence of reaction 4. The small amount of $H_2$ found may have been due to some undeuterated methanol. Because $CH_3OH$ has a higher extinction coefficient at 185 nm than does $CH_3OD$ the presence of some $CH_3OH$ would have a disproportionately higher effect on the isotopic composition of the hydrogen formed.

The two major processes are thus reactions 1 and 2. We have seen that the methoxyl radical formed in reaction 1 cannot contribute to the formaldehyde yield. Therefore $\phi(CH_2O)$ should be the measure of the quantum yield of reaction 2. This conclusion is subject to two reservations. Firstly, it has been shown in the photolysis of *tert*-butyl alcohol that excited alcohols can, in principle, undergo a reaction that leads to hydrogen and to an ether.[27,34] The equivalent reaction written for the methanol case would yield formaldehyde hemiacetal (reaction 16). This compound, however, is not stable and would have been analyzed as formaldehyde. Secondly, if $CH_2O$ in reaction 2 is formed in its $n-\pi^*$ excited state, as suggested by the strictly adiabatic calculations, some of it might well react with methanol by hydrogen abstraction, whereby two hydroxymethyl radicals would be formed (reaction 17) which will end up as ethylene glycol (reaction 11).

$$CH_3OH^* + CH_3OH \rightarrow CH_3OCH_2OH + H_2 \quad (16)$$

$$CH_2O^* + CH_3OH \rightarrow 2{\cdot}CH_2OH \quad (17)$$

To our knowledge, the efficiency of reaction 17 has not been established but is expected to be far below unity.

## IV. Experimental Section

Both the deuterated and the undeuterated methanol employed in this study was fractionated until free of gas chromatographically detectable impurities as well as of formaldehyde. Methanol (2 mL) was poured into a Suprasil QS cell fitted with a gas inlet device[35] that allows the sample to be freed of air by purging it with argon. Complete removal of oxygen is achieved after 20 min. Irradiation was accomplished by a mercury low-pressure arc lamp (of which only the 185 nm quanta are active in this system) at dose rates of $2.8 \times 10^{16}$ or $0.67 \times 10^{16}$ quanta/s received by the sample. Conversions did not exceed 0.1%.

The gaseous products were determined gas chromatographically, being swept out of the solution into a flask from which methane, ethane, and carbon monoxide (the latter after on-line catalytic reduction to methane) were measured by flame ionization; the hydrogen was swept directly into the gas chromatograph by the carrier gas and measured by thermal conductivity.

As regards the hydrogen determinations, the gas chromatograph was calibrated for $H_2$ and $D_2$ but not for HD, which was unavailable. To estimate the HD yield the following procedure was employed: the ratio of the GC response ($R$) to equal volumes of $H_2$ and $D_2$ was determined, and it was found that $R(H_2)/R(D_2) = 1.44$. This result is in close agreement with the value one obtains for the ratio of thermal conductivities $(\lambda(H_2)/\lambda(D_2))$ if one makes use of the Eucken relationship,[36] $\lambda/\eta = 2.5\, C_{v,\text{trans}} + C_{\text{intra}}$ ($\lambda$, thermal conductivity; $\eta$, viscosity; $C_{v,\text{trans}}$ and $C_{\text{intra}}$, heat capacities); inserting the appropriate values,[37] one obtains $\lambda(H_2)/\lambda(D_2) = 1.43$. It was then assumed that $\lambda(H_2)/\lambda(HD) = 1.26$, as obtained from the Eucken relationship, would equal the ratio $R(H_2)/R(HD)$. This ratio constitutes a calibration factor for HD with respect to hydrogen, permitting the estimate of the HD yield, it having been established by mass spectrometry that the hydrogen evolved from $CH_3OD$ was ≥98% HD.

Ethanol was determined gas chromatographically by liquid injection.

Determination of ethylene glycol by gas chromatography was also attempted, but the quantum yield values so obtained were unreasonably low ($\phi \leq 0.3$). From material balance considerations, $\phi$(ethylene glycol) + $\phi$(formaldehyde) = $\phi$(hydrogen) + $\phi$(methane) + $\phi$(ethane); i.e., $\phi$(ethylene glycol) = 0.53 would be expected. A conceivable explanation of the discrepancy would be that in the course of sample evaporation in the injection port, some of the ethylene glycol reacts with the formaldehyde methyl hemiacetal (essentially all the formaldehyde in methanolic solution is sequestered in this form) which remains behind together with the glycol after the bulk of the methanol has flash evaporated, forming the even less volatile formaldehyde hydroxyethyl hemiacetal, which defies gas chromatographic analysis.

Formaldehyde was determined spectrophotometrically by the acetylacetone/ammonium acetate method.[38]

## V. Theoretical Interpretation of the Photolysis Results

The experimental results of the last section, particularly the almost complete lack of $H_2$ found in the product analysis of photolyzed $CH_3OD$, demonstrate that scission of an O–H bond is much more readily accomplished than C–H bond rupture when starting from the n → 3s excited state of this system. This preference is easily understandable in terms of the present potential surface calculations, which show a completely repulsive O–H curve (Figure 1) as compared to its C–H counterpart (Figure 3) possessing a well-defined energy minimum. As pointed out in section II, and also in the work of Kassab et al.,[11] this distinction is derived from the fact that the methoxy radical is spatially doubly degenerate whereas the hydroxymethyl radical is not.

The questions why C–O scission appears to be a minor process compared to O–H dissociation and also why a rather large portion of the products consists of formaldehyde in this photolysis are not answered as straightforwardly by the calculations, but nevertheless a firm basis for understanding these aspects also presents itself. Although the C–O and O–H scission processes appear quite similar from the point of view of qualitative MO theory (Figures 2 and 5), two factors not accounted for at that level of approximation combine to change this picture dramatically.

First the Rydberg–valence avoided crossing takes place significantly more sharply in the C–O case (Figure 4), producing a small barrier in the adiabatic potential curve for the lowest singlet excited state of methanol in this instance as compared to a purely repulsive surface for the O–H separation. This effect was not noted at all in the calculations of Kassab et al.;[11] especially the second excited-state curve was not obtained in their work. If nonadiabatic effects are considered, either via the Landau–Zener model[39] (especially for geometries with COH angles exceeding 150°) or through explicit calculation of nuclear coupling matrix elements,[40] it is found that the diabatic representation is more realistic for the C–O scission, according to which the surfaces which are to be traversed are best viewed as corresponding to either pure Rydberg (bound) or pure valence (repulsive) in character (Figure 4).

In addition there is the kinetic energy factor which indicates that even if the repulsive diabatic surface is reached upon excitation a decided preference toward decomposition involving the very light H atom (i.e., O–H scission) will be noted rather than the C–O

(33) Seki, H.; Nagai, R.; Imamura, M. *Bull. Chem. Soc. Jpn.* **1968**, *41*, 2877–2881.
(34) Sänger, D.; von Sonntag, C. *Z. Naturforsch. B* **1970**, *25B*, 1491–1492.
(35) Weeke, F.; Bastian, E.; Schomburg, G. *Chromatographia* **1974**, *7*, 163–169.
(36) Waldmann, L. In "Encyclopedia of Physics"; S. Flügge, Ed.; F. Springer: Heidelberg, 1958; Vol. 12, p 499.
(37) Landolt-Börnstein. "Zahlenwerte und Funktionen", 6th ed.; Springer: West Berlin, 1969; Vol. II, Part 5a, p 23.
(38) Kakač, B.; Vejdelek, J. J. "Handbuch der Photometrischen Analyse Organischer Verbindungen"; Verlag Chemie: Weinheim, 1974; p 257.
(39) Nikitin, E. E.; Zülicke, L. *Lect. Notes Chem.* **1978**, *8*, 150–155.
(40) Buenker, R. J.; Hirsch, G.; Peyerimhoff, S. D.; Bruna, P. J.; Römelt, J.; Bettendorff, M.; Petrongolo, C. In "Current Aspects of Quantum Chemistry, Studies in Physical and Theoretical Chemistry"; Carbo, R., Ed.; Elsevier: Amsterdam, 1981; Vol 21, p 81–97.

scission process in which both the methyl and hydroxyl fragments possess roughly equal masses. The simple classical model discussed in section IIB indicates, for example, that since the ratios between the respective light and heavy fragments are 31:1 and 17:15, the escape velocity is over 5 times greater in the O–H decomposition process. Deuteration at the oxygen atom leads to a slight reduction of the species related to O–H (O–D) scission (that part of the HD or $H_2$ which is due to reaction 1 followed by reaction 6; its quantum yield equals $\phi$(hydrogen) − $\phi$(formaldehyde)), as well as to a definite increase in the species deriving from C–O breaking (methane and ethane), in agreement with the above kinetic argument. The increase (by 42%) in the quantum yields of methane and ethane, i.e., the main products resulting from C–O scission, is actually larger than one would expect on the basis of the simple classical model (31%), which ignores potential energy considerations, thereby supporting the proposition that the different types of avoided crossings computed for the O–H and C–O processes also play a key role in favoring one primary reaction over the other. In particular the likelihood that the lowest excited-state adiabatic surface would be followed in the C–O scission reaction (Figure 4) is also enhanced as the velocities of the various fragments decrease as a result of deuteration; thus, it appears that a combination of both potential energy and dynamic effects is involved in determining the observed product distribution.

Insofar as O–H scission occurs the experiments indicate that reactions 1 and 2 are of comparable importance. In view of the theoretical evidence that the methyl H atoms are much less likely to separate from the n → 3s excited methanol than is the one attached to oxygen, an alternative model for the $H_2$ elimination (reaction 2) suggests itself other than that considered explicitly in section IIA. Instead of a concerted reaction in which both H atoms leave at essentially the same speed, it seems more likely on this basis that the O–H bond is first lengthened and that subsequently the departing hydrogen atom attracts one of the hydrogens attached to carbon. Potential surface calculations exploring this possibility indicate that at least some barrier is still encountered before the C–H bond is broken and the H–H bond begins to be formed in this nonconcerted pathway, but the fact that the lowest two singlet states of $CH_3OH$ become nearly degenerate when the O–H bond length increases to 2.0 Å (Figure 1) does appear to be advantageous in reaching the final products consisting of $H_2CO$ and $H_2$ in their ground ($^1A'$) state, with the initial methanol excited state being of opposite ($^1A''$) symmetry. Rearrangement of the methoxyl system to the hydroxymethyl radical has been calculated to occur with an activation energy of 76.0 kcal mol$^{-1}$ [41] and is thus seen to be a much less likely process than such an $H_2$ elimination reaction, for example. In this view the high departing velocity of the hydroxyl H atom on a completely repulsive surface again strongly promotes such a process in its initial phase. At a certain point the choice simply has to be made between abstracting a second hydrogen atom from another methanol molecule, in which case a hydroxymethyl is formed which ultimately leads to the production of ethylene glycol, or removing a second H atom from the same system, in which case a molecule of formaldehyde results. It is very difficult to be more quantitative about the exact proportions of ethylene glycol and formaldehyde actually formed in the methanol photolysis in this model, but the assumption that the initial step, namely lengthening of the O–H bond, is the same for both processes and the fact that the subsequent removal of the second hydrogen atom attached to a carbon species is likely to be accompanied by roughly the same activation barrier regardless of whether it comes from the same or a neighboring methanol molecule are at least qualitatively consistent with the experimental findings. Deuteration of the hydroxy group would slow down the initial departure of the first hydrogen atom and thus would appear to have the same effect on both the elimination and abstraction reactions for this step, but since the deuteron should stay in the vicinity of the original methanol group longer than the lighter proton there is some ground for expecting the quantum yield of formaldehyde to increase somewhat once the isotopic substitution is introduced. The experiments at hand indicate first and foremost that deuteration has little effect on the quantity of $H_2CO$ being produced in the photolysis, but a slight trend toward increased production does seem to be present, also consistent with the above arguments, though hardly conclusive.

In saturated ethers the O–H scission primary step which plays such a dominant role in the above interpretation of the photolysis experiments of alcohols drops out from consideration, leaving a competition between C–H, C–O, and C–C bond-breaking processes to determine the reaction profile. Since C–C scission can be expected to be characterized by similar potential surfaces and products as for the corresponding C–H process studied in this work, it follows that products resulting from C–O bond breaking would be the most favored for ethers, which as pointed out in the Introduction is consistent with all known empirical findings for the photolysis of such systems. As a result the distinctive behavior exhibited by saturated alcohols and ethers under photochemical decomposition appears to be properly explained in terms of the present theoretical calculations.

**Acknowledgment.** We thank Professors S. Peyerimhoff (Bonn) and W. Thiel (Wuppertal) for stimulating discussions during the course of this work. The computations in this study have been undertaken on the Perkin-Elmer 3242 system of the Sonderforschungsbereich 42 in Wuppertal.

**Registry No.** Methanol, 67-56-1.

(41) Saebø, S.; Radom, C.; Schaefer, H. F., III *J. Chem. Phys.* **1983**, *78*, 845–853.